Sadhana, Vol. 7, Part 2, July 1984, pp. 91–118. © Printed in India.

Influence of time step in the simulation modelling of evapotranspiration

RAMA PRASAD

Department of Civil Engineering, Indian Institute of Science, Bangalore 560012, India

MS received 26 September 1983; revised 2 January 1984

Abstract. Three simulations of evapotranspiration were done with two values of time step, *viz* 10 min and one day. Inputs to the model were weather data, including directly measured upward and downward radiation, and soil characteristics. Three soils were used for each simulation. Analysis of the results shows that the time step has a direct influence on the prediction of potential evapotranspiration, but a complex interaction of this effect with the soil moisture characteristic, rate of increase of ground cover and bare soil evaporation determines the actual transpiration predicted. The results indicate that as small a time step as possible should be used in the simulation.

Keywords. Evapotranspiration; bare soil evaporation; simulation modelling; radiation balance

1. Introduction

Calculation of evapotranspiration is a necessary step in assessing the water budget of a catchment, storage and conveyance capacities in an irrigation project, size of farm ponds etc. The major part of evaporation over large land areas takes place from the leaves of plants or from bare soil, and the rest from open water surfaces like reservoirs. While evaporation from open water can be computed in a relatively straightforward manner that from vegetation and bare soil is more complex because of its dependence on soil properties and moisture supply and being controlled in addition by plant-physiological behaviour. A common approach to solving the latter problem is by first determining the potential evaporation, *i.e.* assuming ample soil moisture supply, and then applying corrections for actual soil moisture, growth stage of plants etc.

1.1 *Review of some evapotranspiration models*

1.1a *Potential evaporation*

(i) *Penman's formula* The energy for the latent heat of vaporization comes from the sun, and the vapour collecting above the evaporating surface is removed by molecular and convective diffusion. The energy for evaporation is the balance of incident shortwave solar radiation and the reflected shortwave radiation, the longwave radiation of the atmosphere and from the evaporating surface itself, and the energy used for photosynthesis. This energy balance H is used in evaporation E, heating of the air K, heating of the material (plant or soil) S and heating of the surroundings of the material C (Penman 1948),

$$H = E + K + S + C. \tag{1}$$

Penman argued that S and C are negligible over a period, and reduced (1) to

$$H = E + K = E(1+\beta), \tag{2}$$

where $\beta = K/E$, the Bowen ratio, and is given by

$$\beta = \gamma(T_s - T_a)/(e_s - e_d), \tag{3}$$

where γ is the psychrometric constant, T_s is the temperature of the evaporating surface, T_a is the temperature of air, e_s is the saturated vapour pressure at T_s and e_d is the partial pressure of vapour in the air. In the absence of direct measurement of radiation balance, Penman used Brunt's equation to determine H from the incident shortwave radiation, the reflection coefficient of the surface, sunshine duration, and the longwave radiation balance dependent on the air temperature, relative humidity and cloud cover. Determination of E from (2) and (3) involves T_s, the surface temperature, which is difficult to measure. Penman therefore eliminated T_s between (2) and Dalton's formula for evaporation (in terms of windspeed, e_s and e_d) and arrived at his "combination" formula:

$$E = (H\Delta + E_a \cdot \gamma)/(\Delta + \gamma), \tag{4}$$

where Δ is the slope of the saturated vapour pressure-temperature curve at T_a,

$$E_a = (e_a - e_d) f(u), \tag{5}$$

e_a is the saturated vapour pressure at T_a, and $f(u)$ is a function of the windspeed. It has been found by several researchers that the following equation given by Taylor and Priestley serves equally well to calculate E:

$$E = 1{\cdot}26 \frac{H\Delta}{\Delta + \gamma}. \tag{6}$$

Equation (6) is similar to (4), without, however, the wind function.

Penman's formula (as applied to crops) is generally taken to give the evapotranspiration from an extensive surface of vigorously growing and amply watered, short (about 10 cm tall) grass. A crop coefficient (multiplier) is necessary to get the potential evapotranspiration of a crop at various stages of its growth. In addition, if the day-time to night-time ratio of wind speeds deviates considerably from 2·0, it needs a wind adjustment coefficient (when daily mean values of weather parameters are used).

Doorenbos and Pruitt (1977) give values of the wind adjustment coefficient (used again as a multiplier of E) as a function of day-time wind speed and the ratio of day-time to night-time speeds, ranging in value from 0·27 to 1·19.

In order to apply Penman's formula for tall crops also, it can be modified to include the resistance to transfer of vapour from within the substomatal cavities to the atmosphere (Thom and Oliver 1977). This modified formula is, however, not in widespread use. Penman's formula is known to underestimate evapotranspiration in arid regions. It is necessary to add an advective term to it, *e.g.* in the western United States (Chang 1968). Sometimes errors of upto 40% are reported (Doorenbos and Pruitt 1977) when daily mean values of the weather parameters are used. A great deal of work has been done on the effect of wind and the wind function (Stanhill 1962; Rijtema 1965; Wright and Jensen 1972; Doorenbos and Pruitt 1977; Cuenca and Nicholson 1982) to be used in (5). The form of $f(u)$ differs from one location to another and changes with the method used to calculate $(e_a - e_d)$ in (5), which is done in at least six

different ways (Cuenca and Nicholson 1982). Doorenbos and Pruitt (1977) have made a detailed analysis of this question and concluded that no single wind function valid for all climates and seasons can be found. They adopted the strategy of using a single linear wind function and applying corrections by means of their wind adjustment factor. An extreme view also exists, based on a regression analysis of lysimeter and weather data, that radiation and temperature account for the variation in potential evapotranspiration to the extent of 94%, wind, humidity etc. having no significant influence (Hargreaves 1983).

Despite all these uncertainties, Penman's formula is considered to be the best among all available formulae. But the fact that it needs data such as sunshine duration, wind and humidity, which are measured normally only at a relatively few important weather stations, has led to the development of several empirical formulae. Three well-known ones among such formulae are discussed in the following section.

(ii) *Empirical formulae: Thornthwaite's formula:* This formula relates the potential evapotranspiration to the mean air temperature. The underlying assumption, in common with many other empirical formulae, is that mean temperature is a measure of other weather parameters like radiation. It was developed by Thornthwaite (1948) from lysimeter and watershed water loss data in central and eastern USA, and reads:

$$E' = 1{\cdot}6\,(10\,T_i/I)^a, \tag{7}$$

where E' is the total evapotranspiration in a standard month of 360 daylight hours, T_i the mean monthly temperature for the ith month in °C,

$$I = \sum_{i=1}^{12} [T_i/5]^{1{\cdot}514}, \tag{8}$$

and

$$a = 0{\cdot}000000675I^3 - 0{\cdot}0000771I^2 + 0{\cdot}01792I + 0{\cdot}49239, \tag{9}$$

E for any given month is obtained from E' by correcting for the actual number of daylight hours of the month.

As with other similar formulae, the Thornthwaite formula works well in regions where temperature and radiation are strongly correlated. In other regions, its predictions are poor (Chang 1968). In central USA, where it was developed, it is found to be more accurate than even the Penman formula. Regions where temperature is not well correlated with radiation (Doorenbos and Pruitt 1977) are, *e.g.* (i) equatorial regions, (ii) small islands and coastal areas where temperature is influenced by the sea rather than by radiation changes, (iii) at high altitudes, where nights are cold despite high day-time radiation and (iv) regions with a wide variability of sunshine duration in some months, such as those with monsoon climates. In such regions, the Thornthwaite formula may be in error by as much as 100%. Unless verified by lysimeters or other more accurate methods, it is not recommended for use even as a guide to agricultural planning (Chang 1968).

The Blaney–Criddle formula: Based on measurements in western USA, Blaney and Criddle (1950) gave the following formula:

$$E = KT_i p, \tag{10}$$

where E is the monthly evapotranspiration in mm, K a crop coefficient, T_i the mean monthly air temperature in °C, and p the monthly percentage of day-time hours in the year.

Like the Thornthwaite formula, (10) also relates E to temperature, in addition to allowing for the day length. This formula also suffers from the same drawbacks as Thornthwaite's formula and is not recommended for use where temperature is poorly correlated to radiation (Doorenbos and Pruitt 1977). The variability of K with crop stage is a unique feature of (10) among all empirical formulae. Experiments have been conducted at Pantnagar in India (Dakshinamurthy *et al* 1973) to determine monthly K for wheat during the season December–April (outside the monsoon period). Fortnightly K values have been determined for a number of crops in Arizona, USA (Erie *et al* 1965). The formula gives accurate results for the semiarid lands of western USA. There is a very wide variability in the K values in the reported literature, even for places with similar T and p but with differing climates. This led Doorenbos and Pruitt (1977) to modify it in the form:

$$E = cp\,(0{\cdot}46\,T_i + 8), \tag{11}$$

where the crop coefficient K has been dropped, and an adjustment factor c is introduced, which depends on the minimum relative humidity, sunshine duration and day-time wind. They use another crop coefficient K_c to allow for the effect of the crop stage.

Makkink's formula: Makkink (1957) gave a formula relating E to incoming radiation R_s, weighted according to air temperature:

$$E = 0{\cdot}61\,\Delta R_s/(\Delta + \gamma) - 0{\cdot}12, \tag{12}$$

Δ and γ have the same meanings as in (4), which (12) resembles. The formula underestimated E in Israel by a factor of 1·49, although the correlation was high (Chang 1968). The discrepency is attributed to the fact that the formula was derived for a humid region, and did not allow for advection of energy which would occur in an arid region.

However, radiation being the primary source of energy for evaporation, Makkink's formula is inherently superior to formulae which depend primarily on temperature. Where measured values of R_s are not available, as is frequently the case, it can be calculated from observations of sunshine duration which are recorded at weather stations:

$$R_s = \left(a + b\frac{n}{N}\right) R_a, \tag{13}$$

where a and b are constants at a given place, n the actual sunshine hours, N the maximum possible sunshine hours, and R_a the Angot radiation. R_a is tabulated in meteorological tables for different latitudes. a and b have respectively the values 0·31 and 0·46 for New Delhi and 0·31 and 0·49 for Madras.

Doorenbos and Pruitt (1977) recommend a modified version of (12):

$$E = c\Delta R_s/(\Delta + \gamma), \tag{14}$$

where c is an adjustment factor which depends on mean humidity and day-time wind. To use (14), therefore, one needs the air temperature and either the measured R_s or sunshine duration, and an estimate of the general humidity and wind levels using which c can be read off from graphs.

1.1b *Actual evapotranspiration when moisture is not limiting* All the formulae discussed above give the potential evapotranspiration for grass, except the original

Blaney–Criddle formula which uses K values specific for crops. When applied for crops, the crop stage, which has a very great influence on the crop evapotranspiration, has to be considered. The model used in the present work (described later in greater detail) accomplishes this by dividing the evapotranspiration into bare soil evaporation (from the unshaded ground area) and transpiration, and estimating the ground cover on each day. Doorenbos and Priutt (1977) have developed crop coefficients K_c (different from the Blaney–Criddle crop coefficient, though bearing the same name) to obtain E_{crop}, the crop evapotranspiration:

$$E_{crop} = K_c E. \tag{15}$$

Four crop stages are identified, namely initial, crop development, mid-season and late stages. K_c depends on the stage as well as the crop, and varies from 0·2 to 1·25, the lower values occurring at the initial and late stages.

1.1c *Influence of soil moisture* The influence of soil moisture on the ratio of the actual evapotranspiration (AET) to E_{crop} is complex, and depends on the soil characteristics, crop type, crop stage and the magnitude of the potential evapotranspiration (PET) itself. As the soil dries, its hydraulic conductivity decreases, and water moves more slowly towards the roots. When the moisture tension becomes too high, AET becomes less than PET. This break-off tension is higher for lower values of PET and vice-versa. It is high for some crops like horsegram (which is why they are "drought-resistant") and low for sugarcane. For a given crop it is higher during the initial and late stages than during the midseason stage.

It is common practice to specify the break-off point in terms of the depletion of the available soil moisture ASM (defined as the difference between field capacity and permanent wilting point). Some crops are assumed to suffer water stress when 25% of ASM is depleted, some others at 50% and the drought-resistant crops at 75% (Dakshinamurthy *et al* 1973). The British Meteorological Office incorporates the influence of soil moisture through the stomatal resistance term in the Penman equation itself (Thompson *et al* 1981). This also simultaneously takes care of the crop height and stage of growth, AET being thus calculated directly from the modified Penman formula. The first 40% of ASM is assumed to be available freely, and AET becomes less than E_{crop} only after this is exhausted. The soil moisture is apportioned conceptually into two reservoirs, the first one containing 40% of ASM and the second the rest. Water from the second reservoir is drawn only after the first becomes empty. Rainfall or irrigation fills the first reservoir to start with, and the excess after it becomes full goes to the second. Doorenbos and Kassam (1979) have attempted to take into account several parameters and have classified crops into four groups. For each group of crops, they specify values of the soil water depletion fraction p depending on the magnitude of E_{crop}. For a range of E_{crop} from 2 to 10 mm/day, p varies from 0·875 to 0·175 depending on the crop group. It is assumed that AET and E_{crop} are equal as long as

$$\text{CAM} \geqslant (1-p)\ \text{ASM}, \tag{16}$$

where CAM is the current available moisture (defined as the difference between the actual soil moisture content and permanent wilting point). Once CAM becomes less than $(1-p)$ ASM, the following relation is assumed to hold, based on work by Rijtema and Abukhaled:

$$\text{AET} = \frac{\text{CAM}}{(1-p)\ \text{ASM}} E_{crop}, \tag{17}$$

i.e. the ratio of AET to E_{crop} is proportional to the available water content in the root zone. In other words, AET varies linearly with the moisture content of the soil. By a simple integration, it can be shown that in the absence of replenishment of soil moisture through irrigation or rainfall, CAM will decrease exponentially with time t:

$$\text{CAM} = (1-p)\,\text{ASM} \cdot \exp\left[-\frac{tE_{crop}}{(1-p)\,\text{ASM}}\right]. \tag{18}$$

This approach is subject to the criticism that p is independent of the soil characteristics. The assumption of linear relationship between AET and soil moisture content should also be investigated further. The present work uses a model based on soil moisture tension as described later.

1.1d *Water balance models* A complete water balance model uses the above models to provide an output which can be used in irrigation scheduling, water budget calculation, planning of water resources projects, crop yield predictions, etc. The model used in the present work is described in the succeeding sections. In this section, two other recent models are summarised.

(i) MORECS. The British Meteorological office uses this model (*viz* The Meteorological Office Rainfall and Evaporation Calculation System) (Thompson *et al* 1981) to estimate evaporation and soil moisture deficit in Great Britain. The country is divided into square grids 40 × 40 km each. Weather parameters from stations within each grid, which are received at Bracknell around 9 A.M. each day, are averaged and used in a modified Penman equation to calculate PET for a range of vegetation covers from bare soil to forest. AET is then obtained considering the soil moisture for three magnitudes of ASM. Daily water balance is then calculated under the various types of cropped surfaces, and also under the average land use for each square, using the relative proportions of the various surfaces in each grid. Finally computer-drawn maps are produced showing the weekly grid averages of weather parameters, PET, AET, soil moisture deficit and the combined surface run-off and groundwater recharge. Printouts are also produced showing the same quantities for individual surface types. The output is distributed by post and to some extent *via* telex, facsimile and Prestel. MORECS outputs of soil moisture deficit were compared with neutron probe measurements at several sites and the agreement was found to be generally good.

(ii) *Water*. This model was developed by Burt *et al* (1981). It uses the Penman formula and generally follows the approach of Doorenbos & Pruitt (1977). Mean monthly values of weather parameters are used as input, and daily values are interpolated from them by fitting spline polynomials. Sowing dates and initial moisture, if not user-prescribed, are estimated based on air temperature and a 1·5 year water balance run respectively. E is then calculated each day by Penman's formula as modified by Doorenbos and Pruitt. The different growth stages are determined for each crop by the accumulated degree-day method, based on experimental results for the crop. Good agreement was found between predicted E_{crop} and lysimeter measurements.

1.2 *Objective and approach of the present work*

Reliable instruments are currently available for direct measurement of shortwave and longwave radiation at a given point in the upward as well as downward directions. A few meteorological stations in the world already have records of mean radiation over

short intervals of time for several years, along with other meteorological data. With such data, H can be calculated directly simply as a balance of the upward and downward radiations without having to use a Brunt-type formula. This gives great flexibility in choosing the time step for simulation.

The work reported here was undertaken to study the effect of the time step chosen in modelling the evapotranspiration of a crop through the growing season, on the results obtained. An evapotranspiration model was run using two time steps, *viz* 10 minutes and one day. The simulations extended over one calendar year, starting about five months before sowing and ending two months after harvest. Two runs were made with the one-day time step for reasons described later. No attempt has been made to examine the merits of the model itself, which was adapted from an existing one. No conclusions regarding the model itself are to be drawn, attention being confined to the effects of the time step used.

2. The data

Ten years of meteorological data recorded at the Nuclear Research Centre at Karlsruhe, West Germany, from 1973 to 1982 were available on magnetic tapes. The data were recorded every 10 minutes by instruments mounted at various heights on a tower, from midnight to the next 24 hr, from 1 January to 31 December of each year. Although many more items of data were available on the tape, only the following were used in the computations: (i) year, month, day, hour and minute to which the record corresponded; (ii) dew point at 2 m height above ground; (iii) air temperature 2 m above ground; (iv) rainfall; (v) 10-minute mean of the combined downward shortwave and longwave radiation, designated as $(S+L)_d$; and (vi) 10-minute mean of the combined upward shortwave and longwave radiation, designated as $(S+L)_u$. There were many gaps in the individual items of data, apparently because the instruments or recording equipment were out of order. The gaps extended over one or more days in certain years. In this respect, the year 1978 was the best, there being relatively fewer missing data. Accordingly the data for 1978 were selected for the computations. Figure 1 shows month-wise the percentage of the time the data on rainfall, temperature and either $(S+L)_d$ or $(S+L)_u$ or both were missing. Table 1 gives the individual dates on which one

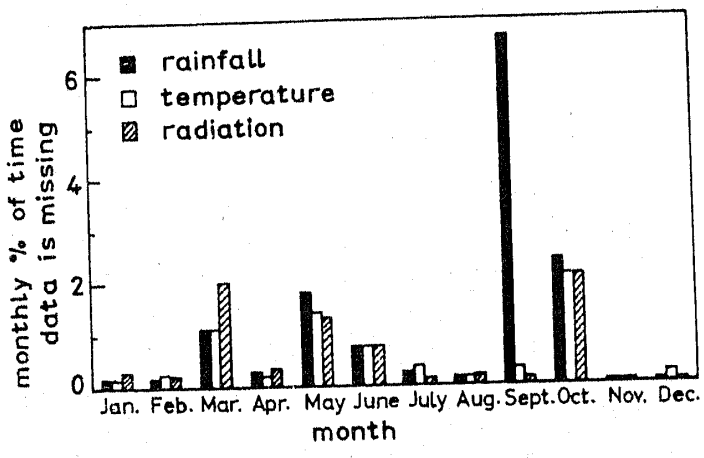

Figure 1. Monthwise extent of missing data

Table 1. Dates on which data are missing for 144 minutes or more

Date	Duration for which data are missing (minutes)
10 March	360
4 May	390
9 May	200
9 June	170
1 September	340
11 September	360
12 September	1090
28 September	210
29 September	500
3 October	240
4 October	170
11 October	650

or more items of data were missing for more than 10 % of the time (*i.e.* 144 minutes). Taking the year as a whole, temperature data is missing 0·58 % of the time, radiation 0·62 % and rainfall 1·2 %. These figures are very small. With the gaps in data filled in as described later (§ 3.2), it can be reasonably assumed that the data is complete.

2.1 *Temperature and dew point*

The air temperature as well as dew point differ by an order of magnitude from summer to winter, as is typical of high latitudes. Figure 2a shows the variation of temperature and dew point (both at 2 m height) on a winter day (1 January) and figure 2b, on a summer day (2 July), from 0 hr to 24 hr. The daily mean value of the air temperature, calculated by averaging all the 144 values of each day, varies through the year as shown in figure 3. The minimum value of the daily mean is −6°C (18 February and 7 December) and the maximum 23·5°C (29 July).

2.2 *Radiation*

Radiation was measured over successive periods of 10 minutes each and the mean value over each period was recorded, in mcal/cm^2/min. The radiation data consist of four values (although only two are used in the computations), *viz* downward shortwave and longwave combined $(S+L)_d$, downward shortwave (S_d), upward shortwave and longwave combined $(S+L)_u$ and upward shortwave (S_u). S_d is the incident solar radiation (direct as well as diffuse), and S_u is that part of S_d which is reflected by the surface. The ratio S_u/S_d thus gives the albedo of the surface (which is grass, under the tower), and $(S_d - S_u)$ is the absorbed shortwave radiation. Both S_u and S_d would be zero during the night.

The absorbed radiaton heats the surface, which consequently emits longwave radiation. The atmosphere, which gets heated by convection, also emits longwave radiation, part of which is reflected by the surface and the rest absorbed. There is thus a longwave radiation exchange between the evaporating surface and the atmosphere which also plays a role in the heat budget. $(S+L)_d$ is the total radiation incident on the

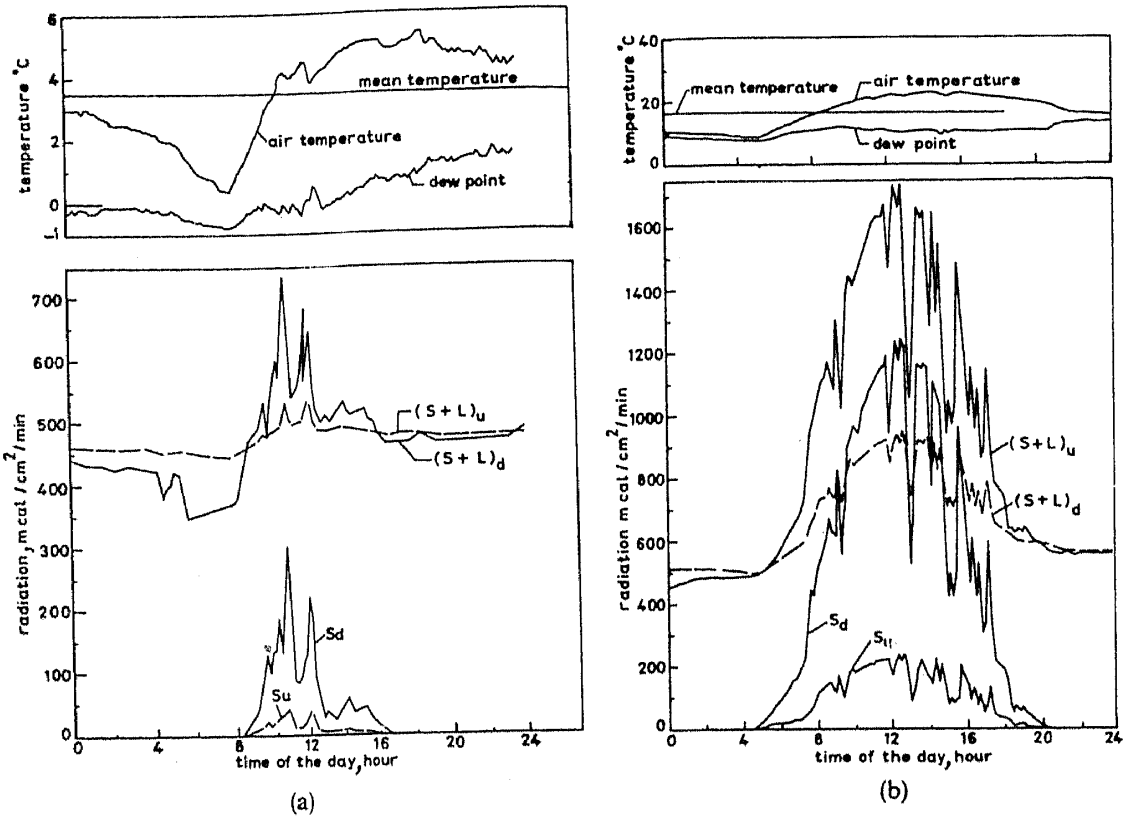

Figure 2. **a.** Variation of temperature, dew point and radiation on 1 January. **b.** on 2 July.

surface, including the longwave emission of the atmosphere. $(S+L)_u$ similarly is the sum of the reflected shortwave and longwave as well as the emitted longwave radiation from the surface. $(S+L)_d-(S+L)_u$ therefore directly gives the energy balance (or net radiation) H occurring in (1). Variations of S_u, S_d, $(S+L)_u$ and $(S+L)_d$ on a winter and a summer day are shown in figures 2a and 2b respectively.

The net radiation is negative on many days, frequently in winter and occasionally during the rest of the year, the site considered being situated at high latitude. During nights it is generally negative. Figure 3 shows the variation of the daily net radiation over the year. Also shown in the same diagram are the negative and positive components of the daily net radiation. These were calculated considering the 10-minute intervals when $(S+L)_d-(S+L)_u$ was negative and positive respectively. As is to be expected, the positive component is much greater than the negative one during summer. In winter they are of similar magnitude. The negative component hovers around an annual mean (of $-23{\cdot}6$ cal/cm^2) throughout the year, but the positive component has a clear plateau in summer. The mean temperature behaves in a similar way, which is the reason why many empirical formulae for evapotranspiration have temperature as their only or the main parameter.

3. Model description

A model being used by van der Ploeg (1983) was adapted for the present study. The original model calculated the net radiation from Brunt's equation using standard data

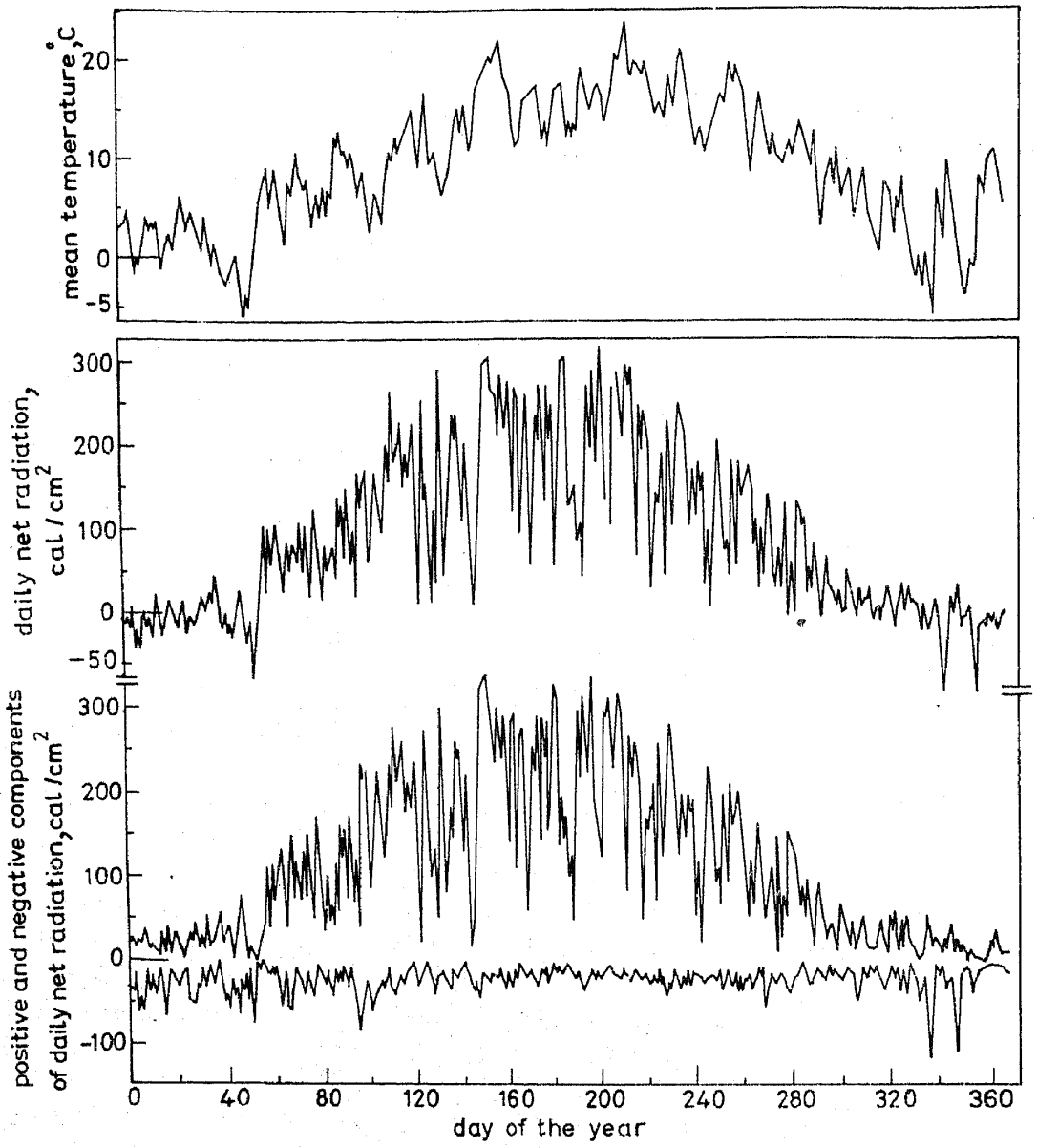

Figure 3. Daily mean temperature, net radiation and its positive and negative components

provided by the German Weather Service. The main modifications made to the model for adaptation here were allowances for (i) direct calculation of the net radiation, (ii) linear variation in the root depth and (iii) transfer of water from the groundwater to the root zone or vice versa depending on the potential gradient. The model uses the Taylor–Priestley equation (equation (6)) to calculate the potential evapotranspiration (PET) from the net radiation. Corrections are applied as described below after first dividing PET into potential evaporation (PE) from soil left uncovered by the plant canopy and potential transpiration (PT) by the plants, to determine the actual evaporation (AE) and actual transpiration (AT). Yield is also determined from the latter.

Figure 4 shows the model flow chart. It starts by reading and storing the soil moisture-tension characteristic, the initial volumetric soil moisture content, the dates of emergence of the seedlings, attainment of maximum root depth and harvest, the

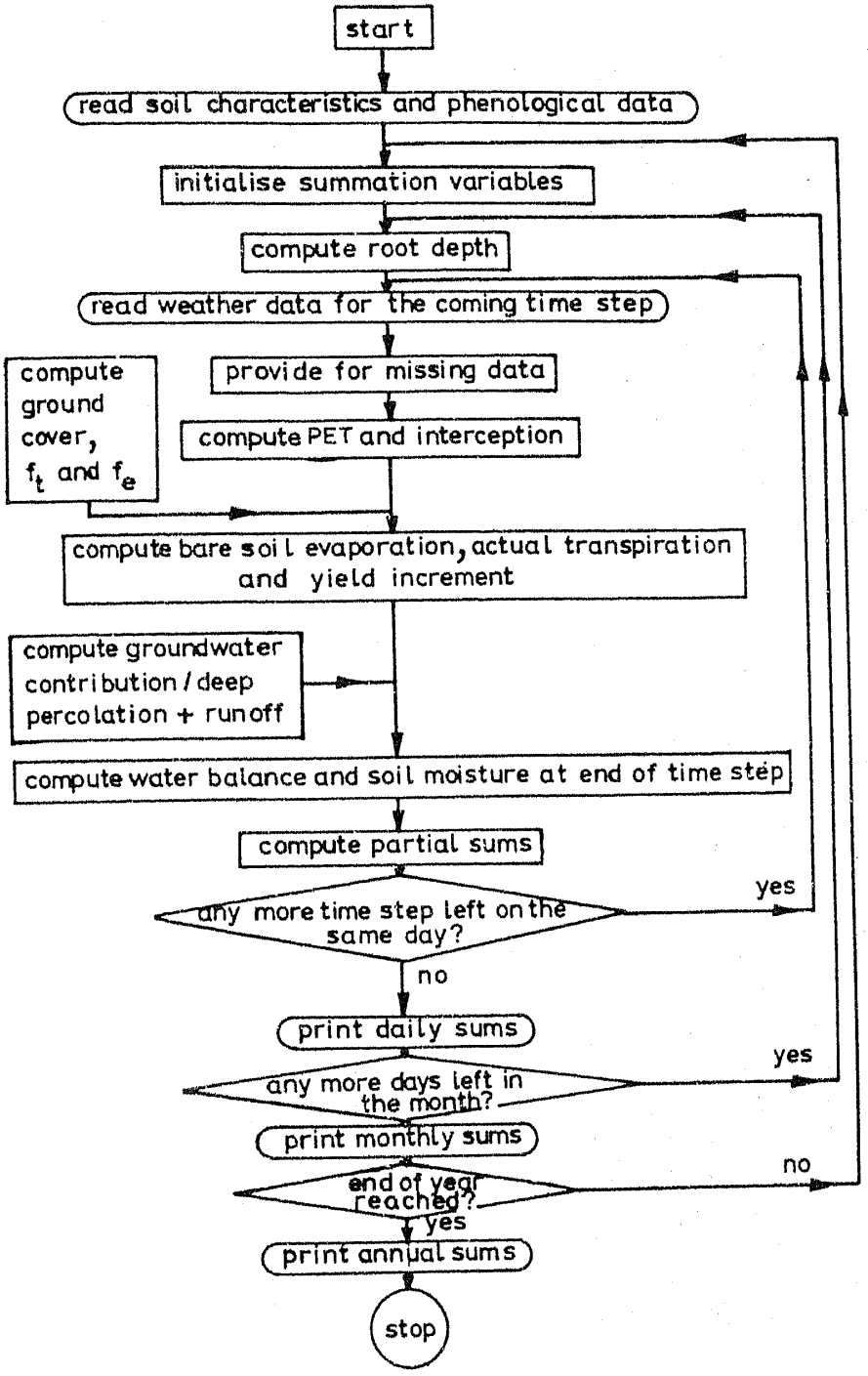

Figure 4. Flow chart of the model

maximum depth of rooting and the depth of the water table. The daily, monthly and annual summation variables are then initialized at zero. Computation starts on 1 January, which is counted as the first day of the year and is carried through to 31 December, the 365th day.

3.1 *Soil depth*

For calculating the soil moisture balance, a depth of soil equal to the rooting depth of the crop is considered. The crop chosen being wheat, maximum root depth was assumed to be 100 cm (Doorenbos and Pruitt 1977). The root depth was assumed to vary linearly from zero to maximum as shown in figure 5 (vide § 4). However, a certain non-zero depth of soil must necessarily be always taken for calculating the soil moisture balance, and this depth is assumed to be 15 cm when the soil is fallow and during the initial period after emergence, as shown in figure 5.

3.2 *Potential evapotranspiration*

The weather data for the current 10-minute period is then read, *viz* dew point and temperature 2 m above ground, precipitation, $(S+L)_d$ and $(S+L)_u$. If data on dew point or temperature were lacking, it would be assumed to be equal to that during the previous 10-minute period. The partial pressure of the vapour in the air is then calculated from the dew point, interpolating from a table of saturated vapour pressure-temperature stored in memory. The net radiation is calculated as

$$H = (S+L)_d - (S+L)_u. \tag{19}$$

If $(S+L)_d$ or $(S+L)_u$ were missing, H would be assumed equal to its value in the previous 10-minute period. The potential evapotranspiration is then computed using the Taylor-Priestley equation

$$E = 1{\cdot}26\,[H\Delta/(\Delta+\gamma)]. \tag{6}$$

Δ is interpolated for the prevailing air temperature from a table stored in memory.

The use of (6) implies that the heat storage terms S (soil) and C (plant and surrounding air) are neglected. In view of the short time step used here, this assumption needs to be justified. The change in stored heat is proportional to the change in temperature. From figures 2a and 2b, it is seen that both during winter and summer, the change in temperature is rapid only during and a little after sunrise, and is relatively slow during the rest of the day. It can therefore be expected that the storage terms are negligible during a large part of the day. The period of interest (here the growing season) is from May to October, when radiation and PET levels are high. The storage terms as a fraction of PET are even more insignificant during this period than in winter. Moreover, once full or nearly full ground cover is established most of the plant mass, the air surrounding it, as well as the soil, will be shielded from direct radiation by the leaves. This will reduce the storage terms even further. As the latitude gets lower and lower, the

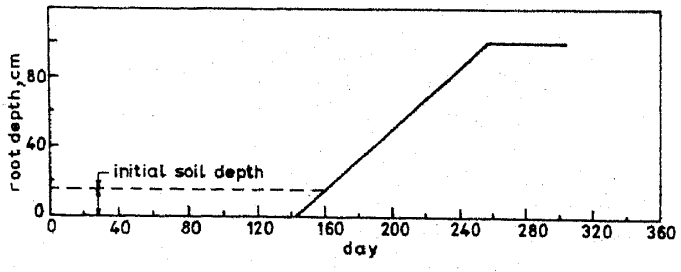

Figure 5. Variation of rooting depth

amplitude of the radiation cycle becomes smaller and smaller, and so do the storage terms. Tanner and Pelton (1960) found the daily soil heat storage term to be around 5% of the net radiation under a good alfalfa-brome cover and 9% under poor cover following cutting. In summer, the values would be much less. According to estimates by Tanner (1960), the storage in the plant mass and surrounding air is even less significant. It is later shown (figures 13a, b, c) that full ground cover is established when only about 10% of the total transpiration of the growing season has taken place, and in view of this and the above considerations, neglect of the storage terms is justified.

3.2a *Negative radiation balance* When the net radiation is negative, with the surface emitting more energy than it receives, the PET calculated as above is negative, meaning that there would be condensation of vapour in the air onto the surface. This is a defect of (6) (not shared by (4)), since condensation occurs only if the surface temperature T_s is less than the dew point and not just whenever the net radiation is negative. If T_s is greater than the dew point, E must be positive, and hence from (2) H can be negative only if $K < -E$. Sensible heat will be flowing from the atmosphere to the surface in such a case, and latent heat in the opposite direction. Figures 2a and 2b show the variation of dew point and air temperature during a winter and a summer day respectively. It is seen that on these two days the air temperature is always greater than the dew point. Since the surface temperature can be expected to differ from the air temperature to a much smaller extent, it is reasonable to assume that the surface temperature is also greater than the dew point. Although this cannot be claimed to be invariably the case, it is true most of the time. Further, during night, the stomata in the leaves would close and transpiration would cease, though PET calculated from (4) might be positive. Moreover, the probability of net radiation being negative during day-time (apart from a short interval of time at sunrise) in the growing season is very small.

In this background, it is convenient to use (6) to calculate E, which is then set equal to zero whenever H is negative.

3.3 *Ground cover*

The PET, when it is positive, is as already stated divided into potential transpiration from the leaf canopy and potential evaporation from bare soil in the proportion of ground cover to exposed bare soil area. The ratio α of the ground cover to the total land area is assumed to vary as follows according to the phenological phases of the crop (vide § 4)

$$\text{Before emergence or after harvest: } \alpha = 0, \tag{20}$$

$$\text{Between emergence and harvest: } \alpha = \frac{1}{1{\cdot}5}(Y + 0{\cdot}001)$$

$$\text{or } 1{\cdot}0, \text{ whichever is less,} \tag{21}$$

where Y is the cumulative dry matter production in tons/ha till the point of time considered, calculated as described in § 3·6. Y increases with actual transpiration (*cf* equation (27)). Ground cover is thus linked to transpiration in the earlier stages, till Y reaches the value 1·499, after which it is assumed that the plant canopy covers the ground completely. The influence of early water stress is thus felt for some time till full ground cover is established. The purpose of the additive constant 0·001 in (21) is to provide for non-zero transpiration in the beginning, so that dry matter production begins from the start.

prediction of a higher transpiration than run 1 in the beginning for all three soils. In Graeusamerwies, aided by a favourable soil moisture tension (*pF* value lies between 2 and 3 for most of the growing season, so that $f_t = 1$), this initial advantage is maintained till harvest. In Hochstetten, it is partly offset later by the effect of too high a moisture content, and by harvest there is only a slight difference between the two runs. In Weichau it is altogether reversed because of the much higher soil moisture of run 3, and transpiration predicted by run 1 is significantly greater.

4.3 *Soil moisture*

For all three soils, run 1 predicts the highest soil moisture depletion, and run 2 the lowest (figure 13). This can be directly attributed to the variations in the predicted bare soil evaporation just prior to full ground cover. As already discussed, run 1 predicts large amounts of evaporation at this stage and as a result, the soil moisture gets to a level favourable to high transpiration, which in turn depletes the moisture further. The low depletion at full cover stage in runs 2 and 3 keeps the soil too moist and leads to a low transpiration factor, which in turn keeps the depletion low during succeeding periods. Only in Graeusamerwies do the soil moisture levels under runs 2 and 3 get into the optimum *pF* range of 2 to 3. A consideration of the moisture characteristics of the soils shown in figure 9 explains why this happens.

The Graeusamerwies soil shows a rapid increase in tension with decreasing soil moisture near saturation, the rate of increase becoming much smaller as the soil dries out a little (just after *pF* crosses 2·2). This characteristic is very favourable from the point of view of the model employed here. A small moisture depletion takes the soil to a state where f_t is 1. Under subsequent full transpiration, the tension increases slowly with decreasing moisture content so that the *pF* value remains less than 3 (the limit beyond which f_t falls, *cf* figure 7) for runs 2 and 3 and does not go beyond 3·25 for run 1. Transpiration takes place at the potential rate (after full cover is established) till harvest for all three runs (except when $pF > 3$ in run 1), and thus this site shows much higher cumulative transpiration than the other two for all runs.

The Weichau soil requires a considerable moisture depletion from saturation for the *pF* to attain the value of 2 (figure 9). Even under run 1 this does not happen except for a short period before harvest (figure 13c). Under runs 2 and 3 the *pF* is way below the 2 mark throughout the growing season.

The Hochstetten soil has an intermediate moisture characteristic (figure 9), and the transpiration also behaves accordingly (figure 13c). Run 1 predicts optimum *pF* values through most of the growing season. For run 2 *pF* remains above 2 for a few days towards the end of September and for run 3 it is less than 2 throughout.

4.4 *Dry matter production*

The cumulative dry matter production predicted by the three runs is illustrated by curves Y1, Y2 and Y3 in figure 13. As already discussed earlier (§ 4·2), the lower saturation deficit in the air assumed by runs 2 and 3 leads to very high yield figures. It clearly swamps the influence of transpiration at Hochstetten and Graeusamerwies, where run 1 predicts the lowest dry matter production. In Weichau, however, due to the very low transpiration predicted by run 2, the yield is lower than predicted by runs 1 and 3. Run 3 predicts the highest yield in all cases, aided partly by the transpiration, but chiefly by the low vapour saturation deficit.

5. Conclusions

The analysis shows that each of the five important quantities in an evapotranspiration model, *viz* potential evapotranspiration, actual bare soil evaporation, ground cover, soil moisture and actual transpiration is influenced by the time step chosen for simulation. The effect of the time step manifests itself through the averaging of quantities like temperature, wind etc (depending on the kind of model used) and the relative magnitudes of positive and negative components of net radiation. The effect is directly felt in the predicted potential evapotranspiration. The effect on the other quantities is indirect, being a result of complex interaction between potential evapotranspiration, rate of dry matter production, bare soil evaporation and soil moisture characteristics. As a result, the actual evapotranspiration does not change in proportion to the PET. In the model used here, variations in the predicted time taken for the establishment of full ground cover play a vital role, in combination with the soil moisture characteristic, in determining the actual transpiration from the potential evapotranspiration. This could be different in other models. If, for instance, it is assumed following usual practice that AET starts decreasing after 50% ASM is depleted, or if full evapotranspiration is allowed under saturation, the results would be quite different in magnitude. While the choice of the present model was dictated purely by considerations of convenience, the present work shows that the influence of the time step chosen for simulation extends much farther than variations in the prediction of potential evapotranspiration. The results point to the need for using as short a time step as possible.

The author records his gratitude to the Alexander von Humboldt Foundation of West Germany for awarding a Fellowship to carry out this work and to the Indian Institute of Science for granting leave for taking up the Fellowship. Thanks are due to the Karlsruhe Nuclear Research Centre and Dr W A Müller for the weather data, Dr A S Machadi for the soil data, Dr H Zaradny for unsaturated hydraulic conductivity values, Dr van der Ploeg for his model for adaptation to this work, Dr C R Prasad for helpful discussions, the University of Hohenheim in Stuttgart for computer and other facilities to carry out the work, and to Sri S A Gangaraju for help in preparing the drawings.

References

Blaney H F, Criddle W D 1950 Determining water requirements in irrigated areas from climatological data. Technical Publication 96 (Washington: US Dept. of Agr.)

Burt J E, Hayes J T, O'Rourke P A, Terjung W H, Todhunter P E 1981 *Water Resources Res.* 17: 1095–1108

Chang J H 1968 *Climate and agriculture* (Chicago: Aldine Pub. Co).

Cuenca R H, Nicholson M T 1982 *J. Irr. Dr. Div. ASCE*: 108IR1 13–23

Dakshinamurthy C, Michael A M, Shri Mohan 1973 *Water resources of India and their utilisation in agriculture* (New Delhi: IARI)

Day W, Legg B J, French B K, Johnston A E, Lawlor W, Jeffers W De C 1978 *J. Agric. Sci., Camb.* 91: 599–623

Doorenbos J, Kassam A H 1979 FAO Irrigation and Drainage Paper No. 33 (Rome: FAO)

Doorenbos J, Pruitt W O 1977 FAO Irrigation and drainage, paper No. 24 (Rome: FAO)

Erie L J, French O F, Harris K 1965 Consumptive use of water by crops in Arizona, Tech. Bull. 169 (Arizona: The University Agricultural Experiment Station)

Feddes R A 1971 *Water, heat and crop growth* (Wageningen: Agricultural University)

Hargreaves G H 1983 *J. Irr. Dr. Div. ASCE* 109IR2: 277–278

Kunze R J, Uehara G, Graham K 1968 *Proc. Soil Sci. Soc. Am.* 32: 760–765

Makkink G F 1957 *Netherlands J. Agr. Sci.* 5: 290–305

Millington R J, Quirk J P 1961 *Trans. Faraday Soc.* 57: 1200–1207
Penman H L 1948 *Proc. R. Soc. (London)*, A193: 120–145
Rijtema P E 1965 An analysis of actual evapotranspiration, Agr. Res. Rep. 659 (Wageningen: Pudoc)
Stanhill G 1962 *Q. J. R. Meteor. Soc.* 88: 80–82
Tanner C B 1960 *Proc. Soil Sci. Soc. Am.* 24: 1–9
Tanner C B, Pelton W L 1960 *J. Geophys. Res.* 65: 3391–3413
Thom A S, Oliver H R 1977 *Q. J. R. Meteor. Soc.* 103: 345–357
Thompson N, Barrie I A, Ayles M 1981 The Meteorological Office rainfall and evaporation calculation system: MORECS (July 1981), Hydrological Memorandum No. 45 (Bracknell: Meteorological Office)
Thornthwaite C W 1948 *Geogr. Rev.* 38: 55–94
van der Ploeg R R 1983 Personal communication
Wright J L and Jensen M E 1972 *J. Irr. Dr. Div. ASCE* 96IR1: 193–201
Zaradny H 1983 Personal communication

3.4 *Potential evaporation from bare soil*

The proportion of the exposed bare soil is $(1-\alpha)$. The model assumes that potential bare soil evaporation is the same fraction of PET:

$$\text{PE} = (1-\alpha)\,\text{PET}. \tag{22}$$

3.5 *Potential transpiration*

The potential transpiration is calculated from α and PET after allowing for the effect of evaporation of that fraction of precipitation which is intercepted by the leaf canopy. As long as there is free water on leaf, the potential drop across the leaf surface necessary for transpiration is absent. The leaf will therefore not transpire till the water on it evaporates. During this time, a corresponding amount of soil moisture will not be extracted by the roots. However, all leaves will neither be simultaneously wet nor covered with equal amounts of water. It is assumed that when intercepted rainwater is still on the leaves, 80% of PET is supplied by it, and the remaining 20% by the soil through transpiration.

The maximum interception for various amounts of rainfall is assumed to follow figure 6, after Feddes (1971). The maximum amount of water that can be held on the leaves is assumed to be 1·92 mm and any precipitation occurring after this would completely reach the ground. If I is the amount of intercepted precipitation retained on the leaves at a given time, and a precipitation P occurs, a further amount I_p is potentially interceptible (figure 6). The actual amount intercepted I_a is determined by a balance of intercepted precipitation, allowing for evaporation equal to 0·8 PET or less depending on the supply, the retention being restricted to a maximum of 1·92 mm:

$$\begin{aligned} I_a &= I_p \text{ if } (I + I_p - 0{\cdot}8\ \text{PET}) \leqslant 1{\cdot}92\ \text{mm};\\ I_a &= (0{\cdot}8\ \text{PET} + 1{\cdot}92 - I)\ \text{mm if } (I + I_p - 0{\cdot}8\ \text{PET}) > 1{\cdot}92\ \text{mm}. \end{aligned} \tag{23}$$

The rest of the precipitation, $(P - I_a)$, would contribute to the soil moisture reservoir and deep percolation and run-off.

The model then calculates the potential transpiration PT, from the difference between PET and direct evaporation of intercepted precipitation, correcting for ground cover:

$$\begin{aligned} \text{PT} &= \alpha[\text{PET} - (I + I_p)] \text{ if } (I + I_p) < 0{\cdot}8\ \text{PET};\\ &= 0{\cdot}2\,\alpha\,\text{PET}, \text{ if } (I + I_p) \geqslant 0{\cdot}8\ \text{PET}. \end{aligned} \tag{24}$$

3.6 *Actual transpiration and bare soil evaporation*

The actual transpiration and bare soil evaporation depend on the soil moisture level. With decreasing soil moisture content, it becomes more and more difficult for the roots

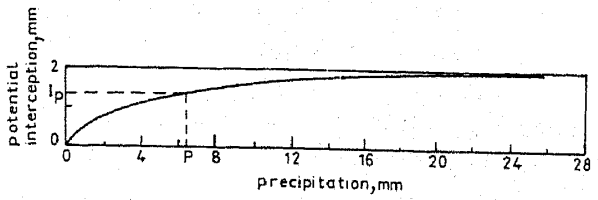

Figure 6. Intercepted precipitation

to extract the water. As the surface soil layer dries out, evaporation from deeper layers also proceeds at a decreasing rate. If the soil moisture is too high (*e.g.* waterlogged condition in the extreme case), while evaporation takes place at a high rate, the root water extraction rate drops again because of the anaerobic environment of the roots. Taking the soil moisture tension, rather than the volumetric soil moisture content, as the more universal indicator of water availability applicable to different soil textures, the model assumes that bare soil evaporation takes place at the potential rate as long as the moisture tension is less than 100 cm, and the rate decreases thereafter logarithmically with increasing tension to zero at 3·5 bars. The transpiration rate is assumed to be equal to the potential rate for moisture tension between 0·1 and 1·0 bar (within which range lies the field capacity, commonly taken to correspond to a tension from $\frac{1}{10}$ to $\frac{1}{3}$ bar). It is assumed to decrease logarithmically with decreasing tension from 0·1 bar till near saturation and again with increasing tension from 1 bar to the permanent wilting point *viz* 15 bars. These assumptions are diagrammatically represented in figure 7, where reduction factors f_e and f_t to be used as multipliers for potential bare soil evaporation and transpiration respectively are plotted against the pF value (defined as $pF = \log_{10} h$, where h is the soil moisture tension in cm of water).

The model determines the soil moisture tension by interpolation from a table stored in the memory, using the soil moisture content at the beginning of the interval. It then determines f_e and f_t and calculates the actual evaporation and transpiration:

$$AE = f_e \cdot PE, \tag{25}$$

$$AT = f_t \cdot PT. \tag{26}$$

The yield increment Y_i during the time interval considered is assumed to be directly proportional to the actual transpiration and inversely proportional to the atmospheric saturation deficit:

$$Y_i = F\left(\frac{AT}{(e_a - e_d)}\right), \tag{27}$$

where F is a proportionality factor, taken here to be 4 tons/ha on the basis of past experience. The form of (27) is supported by past contributions (*e.g.* Doorenbos and Pruitt 1977; Day *et al* 1978). e_a and e_d are calculated by interpolation from stored tables using the air temperature and dew point respectively. The cumulative dry matter production Y is then given by

$$Y = \sum_i Y_i. \tag{28}$$

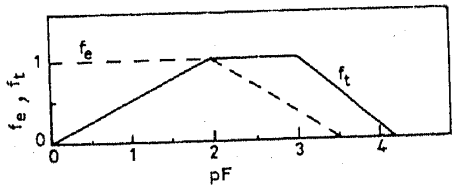

Figure 7. Reduction factors for transpiration and bare soil evaporation

3.7 *Soil moisture*

The soil moisture balance is then calculated from the precipitation reaching the ground, deep percolation and run-off or groundwater contribution to the root zone as the case may be, actual evaporation and actual transpiration.

The root zone of the soil either loses water to the water table by deep percolation or gains from groundwater contribution depending on the direction of the potential gradient, which is determined by the soil moisture tension and depth of the water table. The model assumes that the movement of water in this region obeys Darcy's law, with hydraulic conductivity equal to that in the root zone (figure 8):

$$q = K\left[\frac{d - w/2 - h}{d - w/2}\right], \tag{29}$$

where q is the flux of moisture per unit area (positive downward), K is the hydraulic conductivity of the soil in the root zone at the prevailing moisture content, w the depth of the root zone and d the depth of water table below ground. Equation (29) is obtained by applying Darcy's law between the mid-point in the root zone and the water table. The assumption of constant hydraulic conductivity is strictly not correct, since it varies from the saturated value at the water table to its lower value in the root zone. A more accurate model would have to solve the Richards equation for unsaturated soil moisture movement and that too in the unsteady state. It was, however, considered that the effort would not be worth the results, since during the growing season, the moisture content in the root zone could be expected to be near or less than the field capacity, when the hydraulic conductivity would be quite small. In the extreme case when $K = 0$, there would obviously be no moisture flow into or from the root zone. This condition is satisfied by (29). Equation (29) would again be accurate in the other extreme case when $K = K_s$, the saturated hydraulic conductivity. It was therefore considered that (17) would be adequate.

Positive values of q denote deep percolation and negative values groundwater contribution to the root zone.

The soil moisture balance is now calculated. All inflow and outflow of water is assumed to be uniformly distributed over the root zone depth. The potential increment to the soil moisture, $\delta\theta_p$, is therefore

$$\delta\theta_p = [P - I_a - q - AT - AE]/w. \tag{30}$$

The actual increment would be equal to $\delta\theta_p$ only if the resulting moisture content does

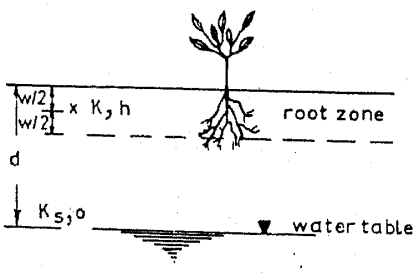

Figure 8. Moisture exchange between root zone and water table

not exceed saturation. Once saturation is reached, additional rainfall will flow over the surface as run-off, Q. Hence

$$\left.\begin{aligned} Q &= (\theta' + \delta\theta_p - \theta_s)\, w, \text{ if } (\theta' + \delta\theta_p) > \theta_s \\ &= 0, \text{ if } (\theta' + \delta\theta_p) \leqslant \theta_s \end{aligned}\right\} \tag{31}$$

where θ' is the soil moisture content at the beginning of the time step and θ_s the saturated moisture content. The moisture content at the end of the interval, θ, is given by

$$\theta = \theta' + \delta\theta_p - Q/w, \tag{32}$$

θ is taken as the initial moisture content for the next interval. q and Q are clubbed together in the output. The summation variables are then updated and calculation for the next interval begins.

4. Computation and results

The simulations were carried out on the VME system (ICL) at the University of Hohenheim. Three sites, situated at Hochstetten, Graeusamerwies and Weichau respectively for which the soil moisture characteristic and saturated hydraulic conductivity were available and which were situated within 10 km of the weather observation tower of the Karlsruhe Nuclear Research Centre, were chosen for the model run. Figure 9 shows the moisture characteristics for the three soils. Unsaturated hydraulic conductivity values were not available for any of the soils. From the values of the saturated hydraulic conductivity and moisture characteristic, values of unsaturated hydraulic conductivity were calculated with a program developed by Zaradny (1983) based on the model of Millington and Quirk (1961) as modified by Kunze *et al* (1968). Figure 10 shows the calculated hydraulic conductivity as a function of moisture content. Selected values of K and θ are highlighted in table 2, *viz* at saturation, 1/3 bar tension (taken as field capacity) and 15 bar tension (permanent wilting point).

In saturated conductivity, the Hochstetten and Graeusamerwies soils are typical of sandy loams and Weichau of medium sand. The conductivity of the Graeusamerwies soil at field capacity is, however, an order of magnitude higher than Hochsttten, and at Weichau, another order of magnitude higher. The moisture contents at field capacity of the three soils differ from each other considerably. The available moisture at

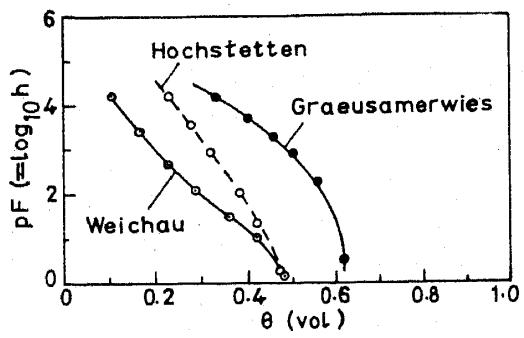

Figure 9. pF-θ curves (h in cm)

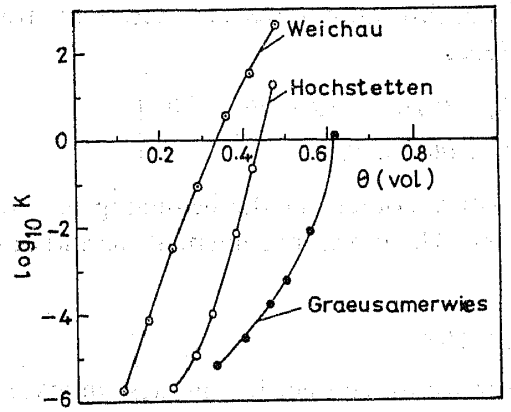

Figure 10. Hydraulic conductivity (K in cm/day)

Hochstetten and Weichau are of the same order (12 % and 14 % respectively), but is significantly higher (21 %) at Graeusamerwies. There is thus considerable variety in the soils chosen for the simulation.

The crop chosen for simulation was wheat. The phenological data were taken from the agricultural statistics for the State of Baden-Wuerttemberg where Karlsruhe is situated. Emergence was assumed to take place on the 143rd day (23 May), maximum root depth to be attained on the 258th day (15 September) and harvest on the 304th day (31 October). As already stated (§ 3·1), the maximum root depth was taken to be 100 cm. The root depth was assumed to increase linearly from zero on the date of emergence to 100 cm on the 258th day, whereafter it remained constant till harvest.

Three simulations were run on each site. The moisture contents measured at the three sites towards the end of December 1980 were taken as typical and given as initial moisture contents at the start of simulation. The first run was made with a time step of 10 minutes.

The second run was made with a time step of one day, using daily mean values of temperature and humidity, total daily net radiation and total daily rainfall. This is the normal kind of data with which most models work and which are provided by weather bureaus, with the exception of radiation (the weather bureaus usually provide the daily sunshine duration, from which net radiation is calculated in most models. The advantage of measured net radiation is made use of here). The total daily net radiation is obtained by summing $(S + L)_d - (S + L)_u$ for all the 10-minute intervals from 0 to 24 hr. When the Taylor–Priestley equation is used, this means that during those 10-minute

Table 2. Soil moisture and hydraulic conductivity at the three sites

	At saturation		1/3 bar tension		15 bar tension	
Site	K cm/day	θ % vol.	K	θ	K ($\times 10^{-6}$)	θ
Hochstetten	68·3	48·6	0·0008	35	2·1	23
Graeusamerwies	27·3	63·2	0·003	54	6·9	33
Weichau	1063·0	49·2	0·011	25	1·9	11

intervals (whether night or day) when net radiation is negative, condensation is assumed. As already discussed (§ 3·2a), this is an error and it is more reasonable to sum over only those intervals of the day when the net radiation is positive.

A third run was therefore made with one-day time step using daily mean temperature and humidity and total daily rainfall as before but only the positive component of the total daily net radiation (figure 3).

4.1 *Potential evapotranspiration*

Figure 11 shows the daily potential evapotranspiration calculated from the Taylor–Priestley equation for the three runs. PET remains small upto about the end of February when it begins to increase and attains a maximum in May. It starts rapidly decreasing towards the end of July and reaches the small winter values about the end of October. This trend is common for all the runs and follows that of the net radiation (as also that of its positive component), and mean air temperature (figure 3), as should be expected. Table 3 gives the cumulative values of PET on the three phenological dates. From the table as well as figure 11, it is clear that the time step used for simulation has a considerable influence on PET. The run using daily mean T and total net radiation (run 2) gives the lowest PET, and that using the 10-minute time step (run 1) the highest. The one-day time step run with only the positive component of net radiation (run 3) gives intermediate values closer to run 1 than to run 2. PET calculation during runs 1 and 3 is

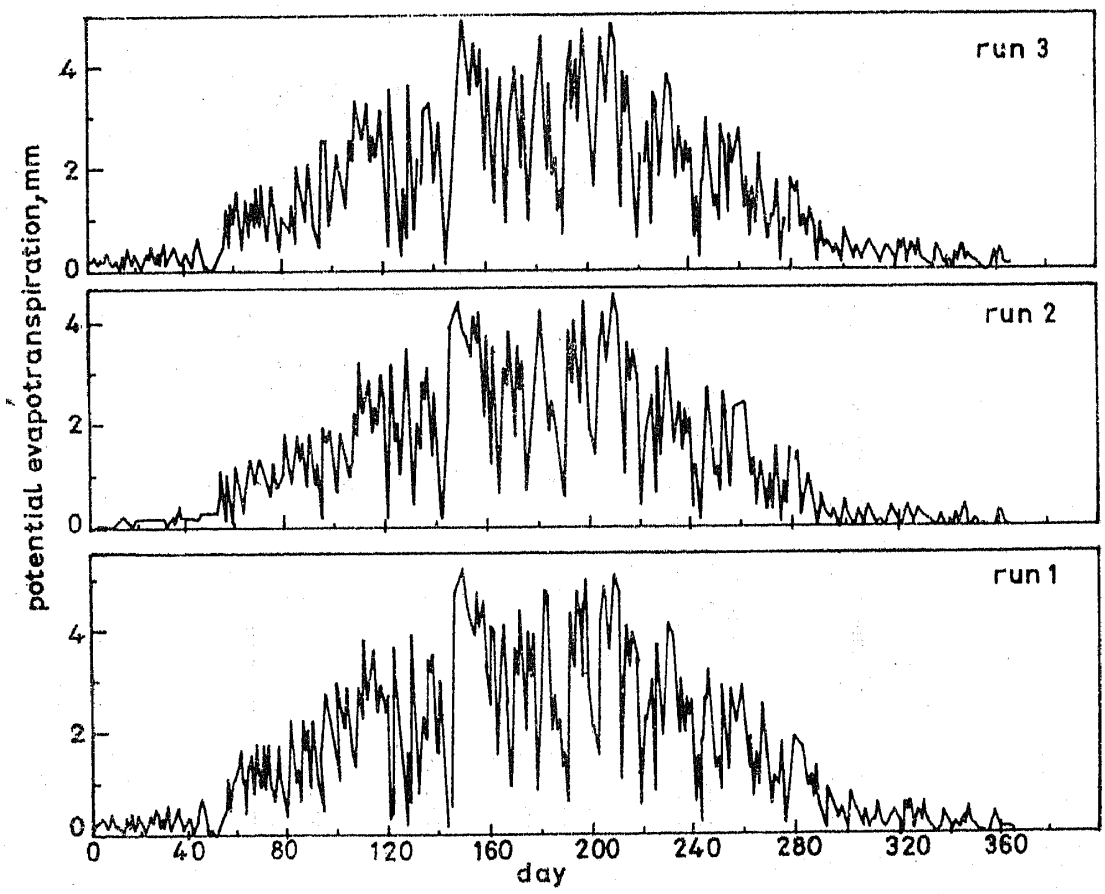

Figure 11. Daily potential evapotranspiration

Table 3. Soil moisture tension and cumulative evaporation and yield at three phenological stages

Date	Simulation Run	PET (mm)	Cumulative values of											
			AT (mm)			*AE* (mm)			*Y* (tons/ha)			*h* (cm)		
			Hoch	Weich	Graeu	Hoch	Weich	Graeu	Hoch	Weich	Graeu	Hoch	Weich	Graeu
	1	172	0	0	0	144	159	134	0	0	0	2	1	4
23 May	2	125	0	0	0	112	123	105	0	0	0	2	1	4
(emergence)	3	157	0	0	0	134	151	126	0	0	0	2	1	4
	1	521	66	70	99	369	398	310	3·80	3·95	5·36	853	114	1348
15 Sept.	2	422	50	35	99	298	330	245	4·36	3·07	8·17	49	11	414
(flowering)	3	481	73	66	132	308	321	247	6·55	5·59	10·85	86	14	648
	1	571	101	106	130	369	398	310	9·13	9·43	10·2	509	85	918
31 Oct	2	457	71	48	124	298	330	245	11·5	7·13	17·0	19	4	231
(harvest)	3	530	106	84	165	308	322	247	17·8	11·8	22·4	42	7	411

confined virtually to day-time, since negative values of PET are set to zero in the former and only the positive component of net radiation is used in the latter.

A source of error in runs 2 and 3 is the fact that the mean daily temperature is used to calculate Δ in (6). The daily mean temperature is obtained simply by taking the arithmetic mean of all the 144 values for the day. From figures 2a and 2b it is seen that most of the net radiation is received when the temperature is near its daily peak. On the other hand, the multiplying factor $(\Delta/(\Delta+\gamma))$ in (6) exhibits a significant variation in the daily range of temperature (figure 12). Figure 2b shows, *e.g.* that on 2nd July the mean temperature is 16·6°C, while the air temperature is 20–22°C when most of the net radiation comes. $\Delta/(\Delta+\gamma)$ is in the region of 0·69 to 0·7 at these temperatures but is equal to 0·64 at the mean. This would account for about 8 % error, which is the order of the difference between run 1 and run 3. Similar orders of magnitude hold for winter too.

An additional source of error in run 2 is the implied assumption in taking the total daily net radiation that moisture is returned from the atmosphere to the crop and soil during nights (and also during the day whenever net radiation is negative) *via* condensation. The PET calculated in run 2 in effect results from subtracting this condensation from the evaporation during the rest of the time. Run 2 therefore always underestimates PET to a greater extent than run 3. One can get from figure 3 an indication of the order of magnitude of the additional error on this account. The negative component of the daily net radiation is comparable in magnitude to the positive upto the end of February and again from the end of October to the end of the year. During this period, run 2 gives very little PET. During the rest of the year, especially in the summer, the positive component is generally much higher than the negative, ignoring exceptional days. Because of this, the cumulative error in PET from run 2 remains within 20 % at the harvest stage. At emergence, however, the compensating effect of summer is only partially felt and the cumulative error is a little more than 27 %, but at flowering it has already come down to 19 %. The total positive component of the net radiation over the year is 735·8 mm equivalent of water evaporation and the total negative component 147 mm, *i.e.* 20 % of the positive component. This is in good agreement with the magnitude of error in PET from run 2.

PET, being dependent only on weather parameters, is the same for all three sites. The actual bare soil evaporation and transpiration are, however, influenced by site characteristics.

4.2 *Actual transpiration and bare soil evaporation*

The actual bare soil evaporation and actual transpiration are both obtained from PET. Evaporation from bare soil takes place along with transpiration only till full ground

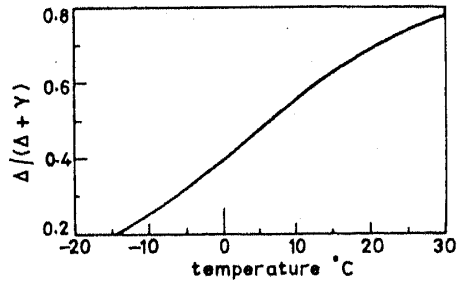

Figure 12. Variation of $(\Delta/(\Delta+\gamma))$ with temperature

cover is established. Subsequently, only transpiration will take place. Bare soil evaporation is obtained using (22) and (25) and transpiration from (23), (24) and (26). The ground cover α depends on the cumulative dry matter production (equation (21)) which depends in turn on the transpiration ((27) and (28)) that has previously taken place. The soil moisture, which is determined by the soil characteristics, previous transpiration and rainfall, also influences current transpiration through the factor f_t in (26). Interpretation of the behaviour of actual transpiration is therefore much more complex than that of PET.

Figures 13a, b, and c show the results produced by the three runs for Hochstetten, Graeusamerwies and Weichau respectively. The bare soil evaporation is depicted by the curves E1, E2 and E3. In each case, run 1 gives the highest cumulative evaporation, with runs 2 and 3 running close to each other, giving about 20 % less than run 1 at harvest

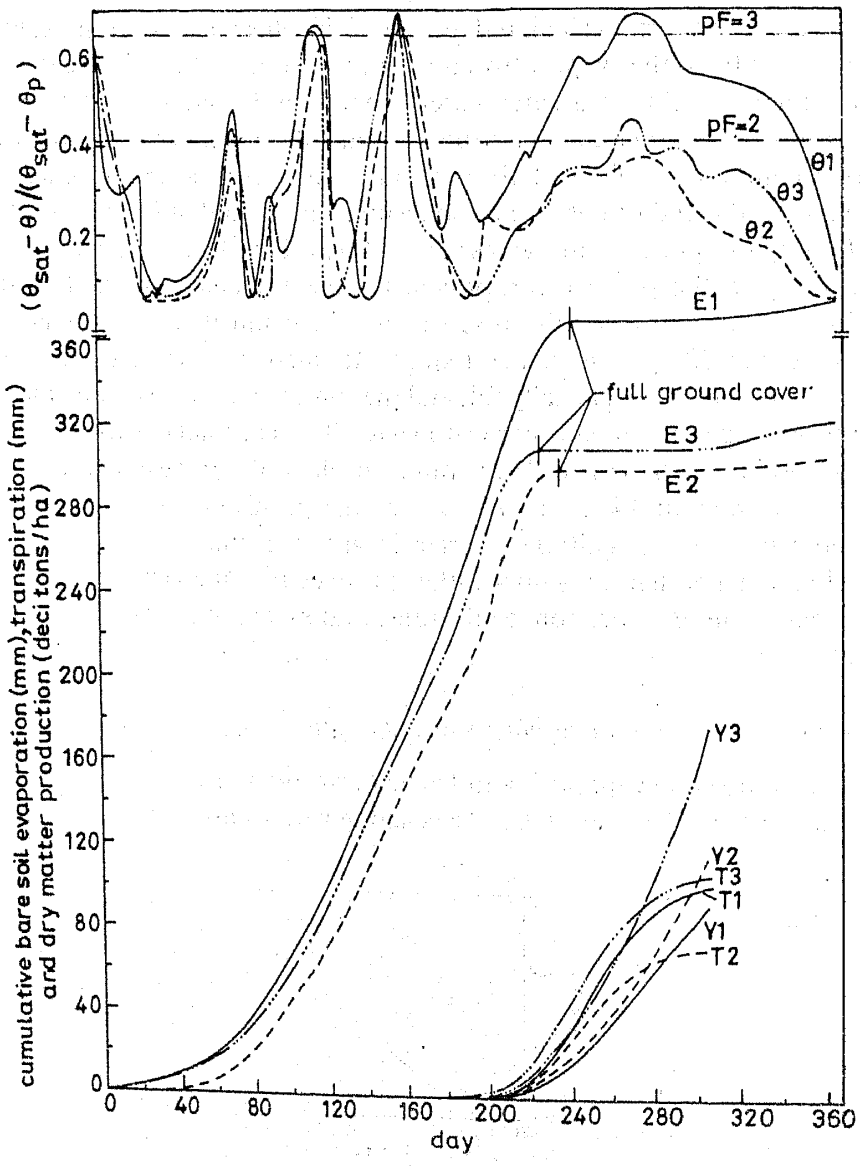

Figure 13a. Simulation results for Hochstetten

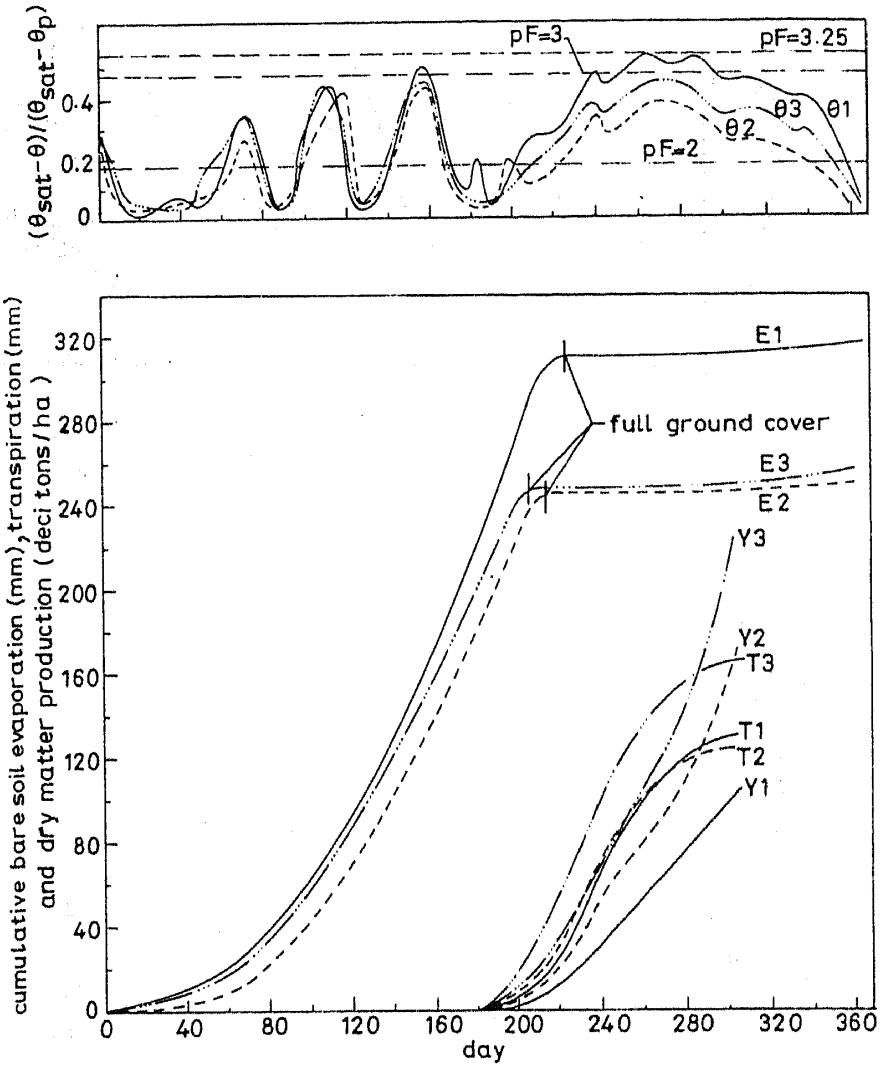

Figure 13b. Simulation results for Graeusamerwies

stage. The large difference between runs 1 and 3 (against only 8 % in PET) is to be traced to the difference in the rates of increase of ground cover between the two runs.

It can be observed that till the end of June (181st day) when the ground cover α is extremely small, the bare soil evaporation values for the three runs are roughly in the same proportion as PET. From emergence onwards, the value of α follows from (21), (27) and (28):

$$\alpha = \frac{1}{1{\cdot}5}\left[F \sum_i \frac{AT}{(e_a - e_d)} + 0{\cdot}001\right]. \tag{32}$$

The actual transpiration and the saturation deficit together determine the ground cover. The influence of the latter will be considered first.

In runs 2 and 3, e_a and e_d are both determined at the daily mean values of the air temperature and dew point respectively. From figure 2b it is seen that on 2 July the mean dew point is around 10°C. (e_d = 12·3 mb) and the mean air temperature 16·6°C (e_a = 18·8 mb). The value of $1/(e_a - e_d)$ for the day in these two runs is therefore about 0·154. In run 1, on the other hand, since essentially daylight values of all quantities are

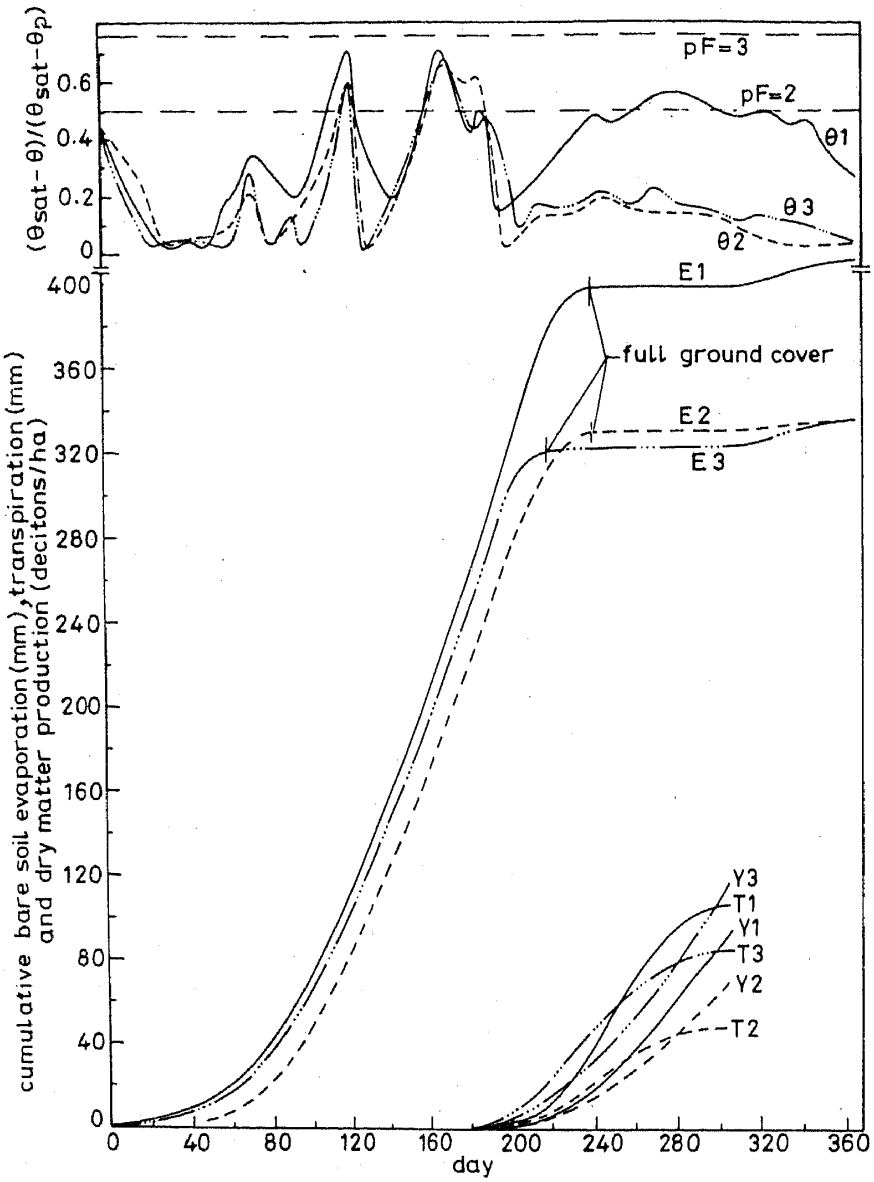

Figure 13c. Simulation results for Weichau

considered, the air temperature is taken around 20°C most of the time. As the dew point varies very little through the day, e_d is still about 12·3 mb, but e_a will be about 23·3 mb. The value of $1/(e_a - e_d)$ for most of the 10-minute intervals will therefore be around 0·091 in run 1. For given cumulative transpiration, therefore, the ground cover calculated in runs 2 and 3 is about 70% greater than in run 1. The influence of transpiration on ground cover is much smaller than that of the saturation deficit, because cumulative transpiration is not significantly large till full ground cover is established.

From (22) and (25), the error induced in AE due to an error in α is given by

$$\frac{d(AE)}{AE} = -\frac{\alpha}{1-\alpha}\frac{d\alpha}{\alpha}. \tag{33}$$

At small values of α, the relative change in AE is smaller than that in α, but as α approaches unity, it is very much magnified. The dates on which full ground cover ($\alpha = 1$) is reached for the three sites under each run are marked across the curves E1, E2 and E3 in figure 13. It is seen that the difference in bare soil evaporation between run 1 and runs 2 and 3 starts rapidly increasing as full ground cover is approached. The increase lasts only for a short time, since evaporation ceases altogether at $\alpha = 1$ (full cover), but it is substantial as it takes place during the summer when PET is high (figure 11).

The difference of about 15% at harvest stage in PET between runs 2 and 3 is not reflected in AE. This is because full cover is reached 10 to 20 days earlier in run 3 due to higher transpiration than run 2. Evaporation from bare soil therefore takes place for a longer duration in run 2 and this compensates to some extent the influence of the lower PET of run 2 as against run 3. It overcompensates, in fact, in Weichau where run 3 yields lower cumulative evaporation at full cover. The overcompensation is due to the extra 21 days of evaporation provided by run 2.

The behaviour of the actual transpiration can now be discussed. The cumulative transpiration is represented by curves T1, T2 and T3 for runs 1, 2 and 3 respectively for each soil in figure 13. In the early stages following emergence, transpiration is influenced by α to a very great extent. As already discussed above, α is higher for runs 2 and 3 than run 1 because of the lower value assumed by the saturation deficit. Therefore runs 2 and 3 give higher values of transpiration (equation (24) than run 1 during the early stages, in spite of their lower PET. Run 3 gives the highest transpiration because the corresponding PET is only 8% lower than that in run 1, compared to 20% for run 2 (*cf* table 3). Very soon, the pattern starts getting influenced by the soil characteristics, through the factor f_t in (26). The soil moisture variation over the year under the three runs is shown by curves $\theta 1$, $\theta 2$ and $\theta 3$ in figure 13, as a plot of the normalised moisture content

$$(\theta_{sat} - \theta)/(\theta_{sat} - \theta_p)$$

against the day of the year. Here, θ is the volumetric moisture content of the soil and the subscripts "sat" and "p" represent the saturation and permanent wilting values respectively. This variable can assume values between 0 (saturated) and 1 (permanent wilting point) and can be described as a "soil saturation deficit". For all three sites it can be seen that during the period when only bare soil evaporation is taking place (upto June), all three runs result in very similar variation of moisture content. Soon after transpiration starts, the trends of variation begin to differ. Run 2 predicts the least transpiration for all three soils. Because of the lower bare soil evaporation during the days just before full ground cover, soil moisture under run 2 is highest at this stage among the three runs. The pF values are marked in figure 13, and it is seen that at full cover stage they are too low, resulting in low values of the transpiration factor f_t (figure 7). Because of this as well as the low PET predicted by run 2, actual transpiration is the smallest for this run, and hence also the draft on soil moisture. The low transpiration level keeps the moisture content high, which in turn keeps the transpiration low. This mutually compounding effect is responsible for run 2 predicting the highest soil moisture contents during the growing season and the lowest transpiration for all three soils. The pF value for Hochstetten and Weichau for run 2 in fact never reaches 2, the minimum necessary for f_t to become unity.

Of the two other runs, the early attainment of full ground cover in run 3 leads to the